Optimum Battery Weight for Maximizing Available Energy in UAV-Enabled Wireless Communications

Hua Yan, *Student Member, IEEE*, Shuang-Hua Yang, Yunfei Chen, and Suhaib A. Fahmy, *Senior Member, IEEE*

***Abstract*—Battery-powered unmanned aerial vehicles (UAVs) have been widely used as enablers of wireless networks. In this letter, the optimal battery weight for UAV-enabled wireless sensor networks is studied. The energy available for communication by considering propulsion energy consumption is maximized. Both numerical and approximate solutions to the optimal battery weight are derived. Numerical results show that both vertical and horizontal flight speeds and the gross weight of the UAV have great impact on the optimal battery weight.**

***Index Terms*—Battery capacity, electric propulsion system (EPS), power consumption, unmanned aerial vehicle (UAV).**

I. Introduction

BATTERY-POWERED electric propulsion systems have been widely used for unmanned aerial vehicles (UAVs) [1]. One challenge for battery-powered UAV communications is the choice of battery weight, as a larger battery weight leads to higher battery capacity for longer flight [3] but also heavier UAV to consume more propulsion power. There may exist an optimal battery weight for the best UAV performance, and this applies to both single and multiple UAV applications [2].

Several works have been conducted on battery-powered UAV electric propulsion systems (EPS). For example, the authors in [4] proposed a systematic design for EPS considering the UAV's payload capacity, flight time and battery pack. In [5], several factors, such as the battery-dumping system and battery packs, were studied to analyse the performance of UAVs. The authors in [6] extended the endurance of battery-powered UAVs by grouping battery packs, and the logarithmic growth trend of durability extension was obtained. In [7], different factors in the design of the EPS for UAVs were investigated. In [8], empirical power consumption models for an Intel Aero Ready to Fly Drone were derived for energy efficient UAV mission planning. All these works have provided very useful insights on the design of battery-powered UAVs. However, none of these works has considered optimal battery weight by accounting for UAV propulsion power consumption, which affects the UAV flight and hence communications performance in practice.

In this work, we study the optimal battery weight in UAV-enabled wireless sensor networks. Both vertical and horizontal flights are considered. Numerical results show that the best battery weight that optimizes the flight performance is determined by the flight height, flight distance, vertical/horizontal flight speed and the gross mass of the UAV excluding battery mass.

(Corresponding author: Shuang-Hua Yang)

H. Yan, Y. Chen and S. Fahmy are with the School of Engineering, University of Warwick, Coventry, U.K. CV4 7AL (e-mail: Hua.Yan@warwick.ac.uk, Yunfei.Chen@warwick.ac.uk and S.fahmy@warwick.ac.uk).

S. Yang is with the Department of Computer Science and Engineering, Southern University of Science and Technology, Shenzhen 518000, China. (e-mail: yangsh@sustech.edu.cn)

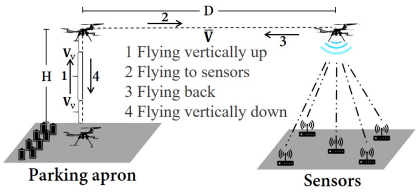

Fig. 1. System model.

II. System Model

Consider the system shown in Fig. 1, where a set of batteries on the parking apron are used as energy for UAV communications. A battery-powered UAV is first equipped with the batteries through an automatic replacement mechanism [9], then flies vertically up to an altitude of H followed by a horizontal flight of distance D to the remote sensors with propulsion consumption, denoted as Stages 1 and 2 in Fig. 1. Upon arrival, the UAV consumes an energy of E_{A2G} for different communications tasks, such as data collection/transmission and wireless power transfer (WPT) [10] – [11]. Finally, the UAV flies back to the parking apron to replace its batteries for the next flight, denoted as Stages 3 and 4 symmetric to Stages 2 and 1, respectively.

In this study, it is assumed that the mass of the UAV, including that of the fuselage and communications system but excluding the battery pack, is m_0, and the mass of the battery pack is m_b. Commonly used lithium polymer (LiPo) batteries are considered because of their high energy density [12]. Thus, the total mass of the UAV is $m = m_0 + m_b$. Using results in [3], [7] and [13], the energy capacity E_b in $W \cdot s$ as a function of the battery mass m_b can be derived as

$$E_b\left(m_b\right) = \rho_e * 3600 * m_b * \eta_{DC-DC},\ 0 \le m_b \le m_{b,max}, \quad (1)$$

where ρ_e is the energy density $(W \cdot hr/kg)$ [3], η_{DC-DC} is the DC-DC conversion efficiency ranging from 0.9 to 0.95 [14], $m_{b,max}$ is the maximum battery mass [7] limited by the rotor thrust.

Remarks: Note that, from [3], the energy density of the LiPo batteries is currently 150 Wh/kg, and can be increased to 250 Wh/kg. We set it to 150 Wh/kg in this work. In the case when the parking apron has a height of H, the vertical flight can be ignored. The following results are still valid by ignoring Stages 1 and 4. Also, in the case when there is no automatic battery replacement mechanism [9], charging through a charging station can be considered.

For the manoeuvring of the UAV, the authors in [15] derived an analytical propulsion power consumption model for rotary-wing UAVs flying at a speed of V with fixed height and rotor

thrust as

$$P\left(V\right)=P_0\left(1+\frac{3V^2}{U_{tip}^2}\right)+P_1\left(\sqrt{1+\frac{V^4}{4v_0^4}}-\frac{V^2}{2v_0^2}\right)^{\frac{1}{2}}+\frac{d_0\rho sAV^3}{2}, \tag{2}$$

where $P_0=\frac{\delta}{8}\rho sA\Omega^3R^3$ and $P_1=(1+k)\sqrt{\frac{(mg)^3}{2\rho A}}$ are two constants related to the physical properties of the UAV and the flight environment, including profile drag coefficient δ, air density ρ, rotor solidity s, rotor disc area A, blade angular velocity Ω, rotor radius R, incremental correction factor to induced power k and gravity acceleration g, U_{tip} denotes the tip speed of the rotor blade, $v_0=\sqrt{\frac{mg}{2\rho A}}$ and d_0 are the mean rotor induced velocity and the fuselage drag ratio, respectively. Details can be found in [15].

For vertical flight, the authors in [16] derived the power consumption model as

$$P_v(V_v,a)=P_2+\frac{T}{2}\left(V_v+\sqrt{{V_v}^2+\frac{2T}{\rho A}}\right), \tag{3}$$

where $T=m\left(a+g\right)$ is the rotor thrust, V_v is the velocity of vertical flight, $P_2=\frac{\delta}{8}\rho sA\Omega^3R^3+k\sqrt{\frac{(mg)^3}{2\rho A}}$, $g=9.8\ m/s^2$ is the gravitational acceleration, $a>0$ is the acceleration for ascending and $a<0$ for descending. We will calculate the propulsion energy consumption using these models.

In general, the performance of a UAV depends on the battery weight m_b. For small m_b, the total mass m is small so that the amount of energy consumed by UAV manoeuvring operations is small. However, the available energy E_b is also small, which results in shorter flight time or less energy for communications. There may exist an optimal m_b.

Denote the transmit power at the UAV as P_{uav-t} in dB. The received power at the ground sensor considering path loss [17] is

$$P_r=P_{uav-t}-\frac{A_0}{1+a_0\mathrm{e}^{-b_0(\theta_0-a_0)}}-B_0, \tag{4}$$

where $A_0=\eta_{LOS}-\eta_{NLOS}$, $B_0=20\lg\left(H\right)+20\lg\left(4\pi f/c\right)+\eta_{NLOS}$, c is the speed of light, θ_0 is the elevation angle, η_{LOS}, η_{NLOS}, a_0 and b_0 are constants related to the propagation environments. The achievable rate in bits/Hz (bs/Hz) is

$$R=\tau\log_2\left(1+\frac{10^{\frac{P_r}{10}}}{10^{\frac{\sigma^2}{10}}}\right), \tag{5}$$

where $\tau=\frac{E_{A2G}}{10^{\frac{P_{uav-t}}{10}}+P(0)}$ is the time for data transmission while hovering, $P(0)$ is the hovering power when the speed is zero ($V=0$ in (2)), and σ^2 is the received noise power at the sensor.

III. Optimization of Battery Weight

In this section, we will maximize E_{A2G} to derive the optimal battery weight. E_{A2G} is given by

$$E_{A2G}=E_b\left(m_b\right)-2\int_0^{T_v}P_v(V_v,a)\ dt-2\int_0^{T_h}P(\overline{V})\ dt, \tag{6}$$

where 2 comes from the symmetric process of Stages 1 and 4, Stages 2 and 3, $T_v=\frac{H}{V_v}+\frac{V_v}{a}$ is the time for ascending in Stage 1 or the time for descending in Stage 4, assumed to be symmetric, $T_h=\frac{D}{\overline{V}}$ is the time for horizontal flight in Stage 2 or 3, $\overline{V}$ is the mean velocity used to calculate the propulsion energy

Algorithm 1: Solving the equation $\frac{\partial E_{A2G}}{\partial m_b}=0$

Input: m_0, H, V_v, a, $\overline{V}$, D, $L_m=0$, M_m, $R_m=m_{b,max}$
if $g(L_m)>0$ && $g(R_m)<0$ **then**
  while $R_m-L_m\le\varepsilon$ **do**
    $M_m=(Float)\left(L_m+R_m\right)/2$
    $g(M_m)>0\ ?\ L_m=M_m:R_m=M_m$
$m_b^*=(Float)\left(L_m+R_m\right)/2$
Calculate E_{A2G} using (7)
Output: m_b^*, E_{A2G}

without considering the acceleration or deceleration, as they are relatively small compared with the long flight at constant speed. The calculation of $\int_0^{T_v}P_v(V_v,a)\ dt$ is divided into three parts, acceleration, constant speed and deceleration, in which the rotor thrust T are $m\left(a+g\right)$, mg and $m\left(g-a\right)$, respectively. Thus, one has

$$E_{A2G}=E_b\left(m_b\right)-E_{vF}-E_{hF}, \tag{7}$$

where

$$\begin{aligned}E_{vF}=&2P_2\left(\frac{H}{V_v}+\frac{V_v}{a}\right)+mg\left(\sqrt{{V_v}^2+\frac{2mg}{\rho A}}\right)\left(\frac{H}{V_v}-\frac{V_v}{a}\right)\\&+m\left(a+g\right)\left(\frac{V_v}{2a}\zeta_1+\frac{m\left(a+g\right)}{a\rho A}\ln\frac{V_v+\zeta_1}{\xi_1}\right)+mgH\\&+m\left(g-a\right)\left(\frac{V_v}{2a}\zeta_2+\frac{m\left(g-a\right)}{a\rho A}\ln\frac{V_v+\zeta_2}{\xi_2}\right),\end{aligned}$$

$$E_{hF}=2\left[P_0\left(1+\frac{3\overline{V}^2}{U_{tip}^2}\right)+P_1\varsigma_1+\frac{d_0\rho sA\overline{V}^3}{2}\right]\frac{D}{\overline{V}},$$

are the total energy for vertical and horizontal flights, respectively, $\zeta_1=\sqrt{{V_v}^2+\frac{2m(a+g)}{\rho A}}$, $\xi_1=\sqrt{\frac{2m(a+g)}{\rho A}}$, $\zeta_2=\sqrt{{V_v}^2+\frac{2m(g-a)}{\rho A}}$, $\xi_2=\sqrt{\frac{2m(g-a)}{\rho A}}$ and $\varsigma_1=\sqrt{\sqrt{1+\frac{\overline{V}^4}{4v_0^4}}-\frac{\overline{V}^2}{2v_0^2}}$. To maximize E_{A2G}, one further has

$$\frac{\partial E_{A2G}}{\partial m_b}=\rho_e*3600*\eta_{DC-DC}-\frac{\partial E_{vF}}{\partial m_b}-\frac{\partial E_{hF}}{\partial m_b}, \tag{8}$$

where

$$\frac{\partial E_{hF}}{\partial m_b}=\frac{\sqrt{2}D}{\overline{V}}\left(1+k\right)g\left(\sqrt{\varsigma_2-\overline{V}^2}+\frac{m^2g^2}{2\varsigma_2\rho^2A^2\sqrt{\varsigma_2-\overline{V}^2}}\right),$$

$$\begin{aligned}\frac{\partial E_{vF}}{\partial m_b}=&g\left(\frac{H}{V_v}-\frac{V_v}{a}\right)\left(\sqrt{{V_v}^2+\frac{2mg}{\rho A}}+\frac{mg}{\rho A\sqrt{{V_v}^2+\frac{2mg}{\rho A}}}\right)\\&+\frac{V_v}{2}\left(\zeta_1-\zeta_2\right)-\frac{V_vg}{2a}\left(\zeta_1+\zeta_2\right)+\left(\frac{H}{V_v}+\frac{V_v}{a}\right)\frac{3k\sqrt{mg^3}}{\sqrt{2\rho A}}\\&+\frac{mV_v}{2a\rho A}\left(\frac{(a+g)^2}{\zeta_1}+\frac{(g-a)^2}{\zeta_2}\right)+gH\\&+\frac{2m}{a\rho A}\left((a+g)^2\ln\frac{V_v+\zeta_1}{\xi_1}+(g-a)^2\ln\frac{V_v+\zeta_2}{\xi_2}\right)\\&+\frac{m^2}{a\rho^2A^2}\left(\frac{(a+g)^3}{(V_v+\zeta_1)\zeta_1}-\frac{(a+g)^3}{\xi_1^2}+\frac{(g-a)^3}{(V_v+\zeta_2)\zeta_2}-\frac{(g-a)^3}{\xi_2^2}\right),\end{aligned}$$

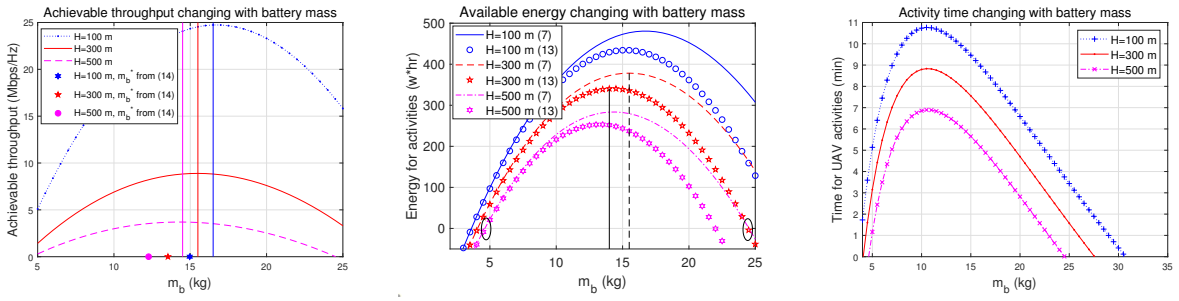

(a) Achievable throughput changing with m_b (b) E_{A2G} changing with m_b (c) Activity time τ changing with m_b

Fig. 2. Throughput, E_{A2G} and τ changing with m_b.

$\varsigma_2 = \sqrt{4v_0{}^4 + \overline{V}^4}$. Taking the second-order derivative of (7), one has

$$\frac{\partial^2 E_{A2G}}{\partial m_b{}^2} = -\left(\frac{\partial^2 E_{vF}}{\partial m_b{}^2} + \frac{\partial^2 E_{hF}}{\partial m_b{}^2}\right), \ 0 \le m_b \le m_{b,max}. \quad (9)$$

Using the energy density of 150 Wh/kg in [3] and the parameters from Table I in [15], it is found that $\frac{\partial^2 E_{A2G}}{\partial m_b{}^2} < 0$, when m_b is between 0 and $m_{b,max} = 20\ kg$ [7]. This implies that the function E_{A2G} has a unique maximum at $m_b = m_b^*$. It is challenging to obtain the exact solution m_b^* by solving the equation $\frac{\partial E_{A2G}}{\partial m_b} = 0$. Denote $g(m_b) = \frac{\partial E_{A2G}}{\partial m_b}$. This can be solved using the binary search in Algorithm 1.

In Algorithm 1, $\varepsilon > 0$ is the given precision tolerance. Thus, its complexity is $O\left(\log_2 \frac{m_{b,max}}{\varepsilon}\right)$. Note that, if $g(L_m = 0) > 0$ and $g(R_m) \ge 0$, E_{A2G} will achieve its maximum at $m_b = R_m$. If $g(L_m = 0) \le 0$ and $g(R_m) < 0$, it will achieve its maximum at $m_b = L_m$, but $m_b = L_m = 0$. Once the maximum energy of E_{A2G} is obtained, the maximum achievable throughput can be derived using (5).

Next, consider an approximation. In (2), $\left(\sqrt{1 + \frac{V^4}{4v_0^4}} - \frac{V^2}{2v_0^2}\right)^{1/2}$ can be approximated as $\frac{v_0}{V}$ by applying the first-order Taylor approximation $(1+x)^{1/2} \approx 1 + \frac{1}{2}x$ when $\left(\frac{v_0}{V}\right)^4 \ll 1$. Then,

$$E_{hF} \approx \frac{2P_0 D}{\overline{V}}\left(1 + \frac{3\overline{V}^2}{U_{tip}{}^2}\right) + \frac{(1+k)\, m^2 g^2 D}{\rho A \overline{V}^2} + d_0 \rho s A \overline{V}^2 D. \quad (10)$$

Also, if the acceleration time during vertical flight is less than that during constant speed, the consumption during vertical flight can be calculated using a mean velocity of $\overline{V_v}$ as

$$E_{vF} \approx \left(2P_2 + mg\overline{V_v} + mg\sqrt{\overline{V_v}^2 + \frac{2mg}{\rho A}}\right)\frac{H}{\overline{V_v}}. \quad (11)$$

Denote E_{vF} as $h(m_b)$ and use the second-order Taylor approximation at $m_b = 0$, one has

$$E_{vF} \approx h(0) + h'(0)m_b + \frac{1}{2}h''(0)m_b{}^2, \quad (12)$$

where $h(0) = \left(\frac{\delta}{4}\rho s A \Omega^3 R^3 + 2k\sqrt{\frac{(m_0 g)^3}{2\rho A}} + m_0 g \overline{V_v} + m_0 g \zeta_3\right)\frac{H}{\overline{V_v}}$, $\zeta_3 = \sqrt{\overline{V_v}^2 + \frac{2m_0 g}{\rho A}}$, $h'(0) = \frac{3kgH}{2\overline{V_v}}\sqrt{\frac{2m_0 g}{\rho A}} + gH + \frac{gH\zeta_3}{\overline{V_v}} + \frac{m_0 g^2 H}{\overline{V_v}\rho A \zeta_3}$ and $h''(0) = \frac{3kgH}{4\overline{V_v}}\sqrt{\frac{2g}{m_0 \rho A}} + \frac{2g^2 H}{\overline{V_v}\rho A \zeta_3} + \frac{m_0 g^3 H}{\overline{V_v}\rho^2 A^2 \zeta_3{}^3}$. Using (10) and (12), (7) can be rewritten as

$$\begin{aligned} E_{A2G} \approx & -\left(\frac{1}{2}h''(0) + \Phi\right)m_b{}^2 - d_0 \rho s A \overline{V}^2 D \\ & + (\rho_e * 3600 * \eta_{DC-DC} - h'(0) - 2\Phi m_0)\, m_b \\ & - \frac{2P_0 D}{\overline{V}}\left(1 + \frac{3\overline{V}^2}{U_{tip}{}^2}\right) - \Phi m_0{}^2 - h(0), \end{aligned} \quad (13)$$

where $\Phi = \frac{(1+k)g^2 D}{\rho A \overline{V}^2}$. From (13), the optimal weight is

$$m_b^* \approx \frac{\rho_e * 3600 * \eta_{DC-DC} - h'(0) - 2\Phi m_0}{h''(0) + 2\Phi}. \quad (14)$$

IV. Numerical Results And Discussion

In this section, numerical examples are given to show the optimal battery mass. In the examples, we set $\rho_e = 150\ Wh/kg$ [3], $\eta_{DC-DC} = 0.9$ [14], $m_0 = 5.5$ kg, $m_{b,max} = 20\ kg$ [7], $a = 2\ m/s^2$, $P_{uav-t} = 40$ dBm, $f = 2$ GHz, $\sigma^2 = -80$ dBm, $D = 40\ km$, $V_v = 4\ m/s$ and $\overline{V} = V = 25\ m/s$. Also, a suburban environment is considered for communication, where $\eta_{LOS} = 0.1\ dB$, $\eta_{NLOS} = 21\ dB$, $a_0 = 5.0188$, $b_0 = 0.3511$ [17], and other parameters of UAV are given in Table I of [15].

Fig. 2(a) shows the achievable throughput versus the battery mass when the flight height changes from 100 m to 500 m. Consider one sensor below the UAV as an example, i.e., $\theta_0 = 0$. One sees that the achievable throughput increases first and then decreases when the battery mass increases. This is consistent with the analysis in Sections II and III. The higher the altitude H, the smaller the optimum m_b and the achievable throughput will be. For example, when $H = 500\ m$, the optimal m_b is about 14.5 kg, which is smaller than 16.5 kg when $H = 100\ m$. This is because larger height consumes extra energy such that E_{A2G} is reduced. For a fixed H, the optimal m_b^* exists indicated by three straight lines. One can see that the values from approximation are smaller than those from Algorithm 1. This is because when $\overline{V_v}$ is set to V_v, the approximation in (12) is larger than the actual value. Meanwhile, the approximation in (10) is also larger than the actual value, thus reducing E_{A2G}.

Fig. 2(b) shows E_{A2G} versus m_b. Similar observations can be made, because the throughput is proportional to E_{A2G} in this case. In this figure, (7) and (13) are used to compare the numerical results of E_{A2G} with the approximate results. Take $H = 300m$ as an example. The gap between the optimal m_b using (7) and the one using (13) is about 1.5 kg, almost consistent with the result in Fig. 2(a). Also, zero-crossing points

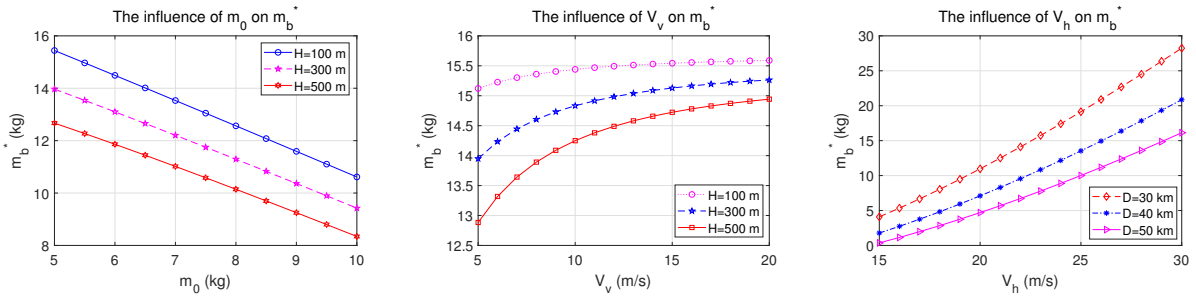

(a) m_b^* changing with m_0 (b) m_b^* changing with V_v (c) m_b^* changing with V_h

Fig. 3. The influence of m_0, V_v and V_h on m_b^*.

marked with ellipse in Fig. 2(b) indicate that $E_{A2G} = 0$ so that the energy provided by the battery can only be used for manoeuvre, not for UAV communications. Note that, for a given task, where E_{A2G} is certain and smaller than the peak value in Fig. 2(b), the optimal battery weight can be obtained by discussing the root of the equation (13) with m_b^* as the unknown.

Fig. 2(c) shows the time for UAV activities using the same parameters as Fig. 2(a) and Fig. 2(b). One can see that, under the same conditions the optimal m_b is about 10.5 kg now, smaller than that in Fig. 2(a) and Fig. 2(b). This means that the optimal m_b for maximum energy does not necessarily maximize time. This can be explained as follows. With larger m_b, more energy is available. However, the power consumption for hovering increases to reduce the hovering time. Therefore, it is important to carefully choose m_b for balanced energy and operation time.

Fig. 3(a) shows the optimal value m_b versus m_0, where H is set to 100 m, 300 m and 500 m. In this figure, (14) is used. One sees that the optimal value m_b decreases with increasing m_0. This is because, when other parameters are fixed, increasing m_0 results in an overall increase in weight, leading to more energy consumption.

Fig. 3(b) shows the effects of V_v on m_b^*. In this figure, (14) is used. One sees that m_b^* increases with V_v first and then approaches an upper limit, which means there should be an optimal V_v that exists for fixed H.

Fig. 3(c) shows how m_b^* changes with V_h. In this figure, H = 300 m and (14) is used. One sees that m_b^* increases with V_h. Taking $D = 40\ km$ as an example, when $V_h = 15\ km/s$, m_b^* is about 2 kg. However, according to Fig. 2(b), the available E_{A2G} is less than 0, and this is meaningless. When $V_h = 30\ km/s$, m_b^* is beyond $m_{b,max} = 20\ kg$. Thus, V_h should be carefully chosen.

V. Conclusion

In this letter, the optimal weight for a battery in UAV electrical propulsion system has been studied. Numerical results have shown that the optimal battery mass that maximizes the flight performance is determined by m_0, vertical/horizontal flight speed V_v/V, flight height H and flight distance D. The larger H and D are, the smaller m_b^* will be. Besides, the optimal battery mass for maximum energy does not necessarily maximize the operation time. Due to the space limitation, several interesting problems remain but will be for future works, such as the joint optimization of transmission power, time and altitude to optimize energy efficiency and the minimization of battery weight for fixed E_{A2G}. Energy efficiency determines the actual use of the maximized available energy and can be optimized via power and time allocation too.

References

[1] "UAV Engine Manufacturers — Propulsion Systems for UAVs, UGVs, AUVs, USVs — Unmanned Systems Technology." https://www.unmannedsystemstechnology.com/category/supplier-directory/propulsion-power/uav-engines-propulsion-systems/.

[2] Z. Yang, C. Pan, K. Wang, and M. Shikh-Bahaei, "Energy Efficient Resource Allocation in UAV-Enabled Mobile Edge Computing Networks," *IEEE Trans. Wirel. Commun.*, vol. 18, no. 9, pp. 4576–4589, Sep. 2019.

[3] J. K. Stolaroff, C. Samaras, E. R. O'Neill, A. Lubers, A. S. Mitchell, and D. Ceperley, "Energy use and life cycle greenhouse gas emissions of drones for commercial package delivery," *Nat. Commun.*, vol. 9, no. 1, pp. 1–13, 2018.

[4] M. K. Mohamed, S. Patra, and A. Lanzon, "Designing electric propulsion systems for uavs," in Lecture Notes in Computer Science (including subseries Lecture Notes in Artificial Intelligence and Lecture Notes in Bioinformatics), 2011, vol. 6856 LNAI, pp. 388–389.

[5] T. Chang and H. Yu, "Improving Electric Powered UAVs' Endurance by Incorporating Battery Dumping Concept," in *Procedia Engineering*, 2015, vol. 99, pp. 168–179.

[6] A. Abdilla, A. Richards, and S. Burrow, "Endurance optimisation of battery-powered rotorcraft," in Lecture Notes in Computer Science (including subseries Lecture Notes in Artificial Intelligence and Lecture Notes in Bioinformatics), 2015, vol. 9287, pp. 1–12.

[7] O. Gur and A. Rosen, "Optimizing electric propulsion systems for unmanned aerial vehicles," *J. Aircr.*, vol. 46, no. 4, pp. 1340–1353, 2009.

[8] H. V. Abeywickrama, B. A. Jayawickrama, Y. He, and E. Dutkiewicz, "Empirical Power Consumption Model for UAVs," in *IEEE Vehicular Technology Conference*, Jul. 2018, vol. 2018-August.

[9] K. A. O. Suzuki, P. Kemper Filho, and J. R. Morrison, "Automatic battery replacement system for UAVs: Analysis and design," *J. Intell. Robot. Syst. Theory Appl.*, vol. 65, no. 1–4, pp. 563–586, Jan. 2012.

[10] H. Yan, Y. Chen, and S.-H. Yang, "Analysis of energy transfer efficiency in UAV-enabled wireless networks," *Phys. Commun.*, vol. 37, p. 100849, Dec. 2019.

[11] H. Yan, Y. Chen, and S.-H. Yang, "UAV-Enabled Wireless Power Transfer with Base Station Charging and UAV Power Consumption," *IEEE Trans. Veh. Technol.*, pp. 1–1, Aug. 2020.

[12] "Li-polymer Battery: Substance or Hype? – Battery University." https://batteryuniversity.com/learn/article/the_li_polymer_battery_substance_or_hype.

[13] M. Gatti and F. Giulietti, "Preliminary design analysis methodology for electric multirotor," in *IFAC Proceedings Volumes (IFAC-PapersOnline)*, 2013, vol. 2, no. PART 1, pp. 58–63.

[14] S. Park, L. Zhang, and S. Chakraborty, "Design space exploration of drone infrastructure for large-scale delivery services," in *IEEE/ACM International Conference on Computer-Aided Design, Digest of Technical Papers, ICCAD*, Nov. 2016, vol. 07-10-November-2016.

[15] Y. Zeng, J. Xu, and R. Zhang, "Energy Minimization for Wireless Communication With Rotary-Wing UAV," *IEEE Trans. Wirel. Commun.*, vol. 18, no. 4, pp. 2329–2345, Apr. 2019.

[16] Z. Yang, W. Xu, and M. Shikh-Bahaei, "Energy Efficient UAV Communication with Energy Harvesting," *IEEE Trans. Veh. Technol.*, vol. 69, no. 2, pp. 1913–1927, Feb. 2020.

[17] A. Al-Hourani, S. Kandeepan, and S. Lardner, "Optimal LAP Altitude for Maximum Coverage," *IEEE Wirel. Commun. Lett.*, vol. 3, no. 6, pp. 569–572, Dec. 2014.